K-Ras-Independent Effects of the Farnesyl Transferase Inhibitor L-744,832 on Cyclin B1/Cdc2 Kinase Activity, G2/M Cell Cycle Progression and Apoptosis in Human Pancreatic Ductal Adenocarcinoma Cells[1]

Si Young Song*, Ingrid M. Meszoely*, Robert J. Coffey[†‡], Jennifer A. Pietenpol[§] and Steven D. Leach*[‡]

Departments of *Surgery, [†]Medicine, [‡]Cell Biology, [§]Biochemistry, The Vanderbilt-Ingram Cancer Center, Vanderbilt University Medical Center and Nashville VAMC, Nashville, TN

Abstract

Pancreatic ductal adenocarcinoma is a highly lethal malignancy that is resistant to traditional cytotoxic therapy. High rates of activating codon 12 K-Ras mutations in this disease have generated considerable interest in the therapeutic application of novel farnesyl transferase inhibitors (FTIs). However, a comprehensive analysis of the effects of FTI treatment on pancreatic cancer cells has not been performed. Treatment of five different human pancreatic cancer cell lines with FTI L-744,832 resulted in inhibition of anchorage-dependent growth, with wide variation in sensitivity among different lines. Effective growth inhibition by L-744,832 correlated with accumulation of cells with a tetraploid (4N) DNA content and high levels of cyclin B1/cdc2 kinase activity, implying cell cycle arrest downstream from the DNA damage-inducible G2/M cell cycle checkpoint. In addition, sensitive cell lines underwent apoptosis as evidenced by changes in nuclear morphology and internucleosomal DNA fragmentation. L-744,832 at a concentration of 1 μM additively enhanced the cytotoxic effect of ionizing radiation, apparently by overriding G2/M checkpoint activation. The effects of FTI treatment on cell growth and cell cycle regulation were associated with changes in posttranslational processing of H-Ras and N-Ras, but not K-Ras. The results confirm the potential therapeutic efficacy of FTI treatment in pancreatic cancer, and suggest that farnesylated proteins other than K-Ras may act as important regulators of G2/ M cell cycle kinetics. *Neoplasia* (2000) **2**, 261–272.

Introduction

Many cellular proteins require posttranslational prenylation for full biologic activity. At least three prenylating enzymes are present in mammalian cells. Among these, protein farnesyl transferase (FTase) and protein geranylgeranyl transferase type I (GGTase-I) represent structurally related heterodimers sharing a common α-subunit (reviewed in Refs. [1,2]). FTase catalyzes transfer of a 15-carbon farnesyl moiety to the C-terminal CAAX motif of multiple protein targets, including H-Ras, N-Ras, K-Ras, Rap2, RhoB, lamin A and B, and the phosphotyrosine phosphatases PRL-1/PTP-CaaX-1 and -2. FTase activity is maximal for CAAX sequences ending in serine, methionine, or glutamine. In contrast, the structurally related enzyme GGTase-I modifies target proteins by addition of a 20-carbon geranyl-geranyl isoprenoid group, with kinetics favoring CAAX motifs ending in leucine. Well-known GGTase-I targets include Rho, Rap and Rac family members, G-protein γ-subunits, and Cdc42. Additional complexity is provided by examples of RhoB farnesylation by GGTase-I [3], and alternative GGTase-I mediated geranylgeranylation of normally farnsylated K-Ras [4]. In contrast, GGTase-II represents a structurally unrelated protein that prenylates non-CAAX peptide motifs [5].

Among target proteins for these enzymes, the Ras proto-oncogene family has been extensively characterized [6,7]. Ras family genes encode 21-kDa guanine nucleotide-binding proteins that transduce signals controlling cellular proliferation and differentiation. In normal cells, Ras switches between inactive GDP-bound and active GTP-bound states. Mutations that stabilize the active GTP-bound state have been identified in over 30% of human tumors, with particularly high incidence in carcinomas of the pancreas and colon [8,9]. For Ras members to transduce either normal or oncogenic signals, a series of FTase-initiated posttransla-tional modifications must occur. Farnesylation on the cysteine residue of the C-terminal CAAX box is followed by peptidase removal of the "AAX" tripeptide and methylation of the resulting cysteine carboxylate. These modifications appear to be required for membrane association and down-stream signaling, including recruitment of Raf kinase to the plasma membrane [10,11].

Examination of farnesylation-dependent events involving Ras and other cellular proteins has been facilitated by the development of specific peptidomimetic inhibitors of FTase. Many of these compounds have been identified based on strategies of rational drug design directed at development of novel cancer therapeutics. In this regard, the potential utility of FTase inhibitors (FTIs) has been supported by extensive preclinical evaluation, demonstrating potent antiproliferative effects on Ras-transformed cells *in vitro* and *in vivo*, with little effect on normal cells [12–18]. These findings have resulted in the initiation of clinical trials of FTI, including evaluation in patients with pancreatic cancer.

In the United States, pancreatic cancer afflicts 29,000 patients per year, with an overall 3-year survival rate of 3%. This high frequency and poor prognosis combine to make pancreatic cancer the fifth leading cause of cancer death in the United States [19]. In addition to this poor prognosis, pancreatic cancer demonstrates the highest known rate of Ras activation among human tumors, with codon 12 mutations identified in at least 90% [8,9]. Combined with a notoriously poor response to traditional therapies [20], these features suggest that pancreatic cancer may represent an ideal target for FTI therapy. Several prior studies suggest that inhibition of Ras function may alter the growth characteristics of pancreatic cancer cells [21–23]. However, a comprehensive analysis of the effects of FTIs on pancreatic cancer cell proliferation, survival, and cell cycle regulation has not yet been performed. In addition, the ability of FTIs to alter farnesylation of different Ras family members in pancreatic cancer cells has not been assessed.

In the present study, we have characterized the growth inhibitory effect of the FTI L-744,832 against five different human pancreatic ductal adenocarcinoma cell lines with and without activating K-Ras mutations. These cell lines exhibited a broad range of sensitivity to FTI, with $IC_{50}s$ ranging from 1.3 to >50 µM. For all cell lines, growth inhibition was associated with accumulation of cells with a tetraploid (4N) DNA content, suggesting alterations in G2/M cell cycle progression. In spite of high levels of cyclin B1/cdc2 kinase activity, FTI-treated cells showed no tendency to form mitotic spindles, suggesting a defect in mitotic progression. For cell lines sensitive to L-744,832, FTI treatment was associated with induction of apoptosis as well as additive cytotoxicity when combined with ionizing radiation. Biochemical analysis revealed changes in post-translational modification of H-Ras and N-Ras, but not K-Ras. The results confirm a potential therapeutic effect of FTase inhibition in pancreatic cancer, and suggest that the growth inhibitory effects of FTI may involve targets other than activated K-Ras.

Materials and Methods

Primary and Secondary Antibodies

The following antibodies were used: rabbit anti-H-Ras, rabbit anti-N-Ras, mouse-anti cyclin B1, mouse-anti cdc2,

horseradish peroxidase-conjugated anti-mouse and anti-rabbit secondary antibodies were purchased from Santa Cruz Biotechnology. Rabbit phospho-specific anti-Cdc2 (Y15) was purchased from New England Biolabs. Mouse anti-K-Ras was purchased from Calbiochem. For immuno-fluorescent staining, rat pan-Ras Y-13,258 antibody and Cy3 donkey anti-rat secondary antibody were purchased from Jackson ImmunoResearch.

Cell Lines and Culture Conditions

Five different human pancreatic ductal adenocarcinoma cell lines were used: Aspc-1, Bxpc-3, Capan-2, Cfpac-1, and Panc-1. These cell lines demonstrate a variety of genetic alterations with respect to K-Ras mutation, p53 mutation, and p16 deletion [8,9,24,25]. Specifically, all cell lines with the exception of Bxpc-3 carry activating mutations in codon 12 of the K-Ras proto-oncogene. In addition, all cell lines with the exception of Capan-2 carry inactivating mutations involving the p53 tumor suppressor gene. Cell lines were obtained from American Type Culture Collection (Rockville, MD). Aspc-1 and Bxpc-3 cells were grown in RPMI medium 1640 (Gibco BRL), Capan-2 in McCoy's 5A medium (Gibco BRL), Cfpac-1 in Isocove's modified Dulbecco's medium (Gibco BRL), and Panc-1 in DMEM (Gibco BRL), supplemented with 10% fetal calf serum, 100 units/ml penicillin, and 100 mg/ml streptomycin at 37°C in an atmosphere of 95% air and 5% CO_2.

FTI Treatment and Anchorage-Dependent Growth Assays

The peptidomimetic FTI L-744,832 was provided by Allen Oliff (Merck Pharmaceuticals, West Point, PA). To evaluate dose-dependent growth inhibition, cells were plated in six-well plates at a density of 1×10^4 cells/well. Twenty-four hours later, cells were treated with 0.1% DMSO vehicle control or escalating doses of L-744,832 ranging from 100 nM to 50 µM. Medium containing fresh DMSO or FTI was replaced at 24-hour intervals. Assessment of growth inhibition was performed at 24, 48, and 72 hours by trypsinization and counting of quadruplicate plates. Cell viability was confirmed by trypan blue dye exclusion. IC_{50} values were established by determining the concentration of L-744,832 associated with a 50% reduction in cell number compared to DMSO-treated control cells at 72 hours.

Cell Growth Following Ionizing Radiation

To determine the effect of FTI on cell survival following ionizing radiation, Panc-1 cells were plated in six-well plates as described above, and exposed to escalating doses of ionizing γ-irradiation (1 to 8 Gy) delivered by a cesium source. Immediately following radiation, cells were treated with either 0.1% DMSO or escalating doses of FTI (0.1 to 10 µM). Medium containing fresh DMSO or FTI was replaced at 24-hour intervals. Cell survival was assessed at 2, 5, and 7 days by trypsinization and direct counting of triplicate plates for each condition.

Cell Cycle Analysis by Flow Cytometry

Flow cytometry was performed as previously described [26]. Briefly, unsynchronized pancreatic cancer cell lines were seeded at 5×10^4 per T25 flask and exposed to different concentrations of FTI as described above. Following treatment, cells were incubated with trypsin/EDTA, washed twice with PBS, mechanically dispersed using 21-gauge needle, and fixed in ice-cold 100% ethanol. After overnight fixation, 1×10^6 cells were resuspended in PBS containing 1 mg/ml RNase and 1 mg/ml propidium iodide. Cell cycle analysis was performed using a FACScan flow cytometer (Becton Dickinson). For each condition, the cell cycle distribution of at least 10,000 cells was analyzed.

Cyclin B1/cdc2 Kinase Assay

Immunoprecipitation-based assay of cyclin B1-associated kinase activity was performed using a mouse monoclonal anti-cyclin B1 antibody (Santa Cruz Biotechnology) and exogenous histone H1 substrate, as previously described [26,27]. Reaction products were resolved on SDS–10% polyacrylamide gels, stained with Coomassie blue, and dried. Incorporation of radioactive phosphate into histone H1 was visualized by autoradiography, quantified using an Instant Imager (Packard Instruments), and expressed as percentage of DMSO-treated control conditions. Data from three independent experiments were pooled and statistical comparison was performed by paired t-test.

Protein Extraction and Immunoblotting

Following treatment with 10 µM of FTI or DMSO for 48 hours, cells were scraped from culture flasks and washed in PBS. For the detection of cell cycle regulatory proteins, whole cell lysates were prepared for immunoblotting as previously described [26]. For the detection of K-, H-, and N-Ras, crude membrane fractions were prepared. Cells were suspended in 0.9 ml of ice-cold hypotonic buffer (25 mM Tris–HCl, pH 8.0, 1 mM EDTA, 5 mg/ml leupeptin, 1 mM Pefabloc SC, 50 mg/ml aprotinin, 5 mg/ml soybean trypsin inhibitor, 4 mM benzamidine) and sonicated for 5 seconds. The cell debris was pelleted and discarded, and the supernatant was transferred to Beckman polyallomer tubes and spun at 46,000 rpm (100,000g) for 45 min. Pellets were washed once with ice-cold hypotonic buffer in the presence of protease inhibitors, re-pelleted at 46,000 rpm for 15 min, then resuspended in 200 µl of ice-cold hypotonic buffer with protease inhibitors. Following electrophoresis of 50 µg protein samples on 13% SDS–polyacrylamide gels, immunoblotting was performed on PVDF membranes (Immobilon-P, Millipore).

Immunofluorescent Staining for Pan-Ras and TdT Labeling

Cells were plated on eight-chamber slides (Nalge Nunc International) and treated with DMSO or 10 µM FTI for 48 hours. For indirect immunofluorescent staining, the cells were rinsed with ice-cold PBS and fixed in 2% paraformaldehyde in PBS for 20 min at 4°C. After washing in ice-cold PBS, cells were incubated with anti-rat pan-Ras primary antibody in PBS with 0.02% saponin for 1 hour at 4°C. Cells were washed again with ice-cold PBS and incubated with donkey anti-rat Cy3 conjugated secondary for 20 min in the dark, then counterstained with 4,6-diamidino-2-phenylindole (DAPI).

For TdT labeling, *in situ* labeling of apoptosis-induced DNA fragments was performed using fluorescein ApopTag Direct *In Situ* Apoptosis Detection Kit (Oncor). Cells were treated and fixed as described above, and then stained according to the manufacturer's instructions. Briefly, cells were incubated with equilibration buffer for 5 minutes, then incubated with TdT enzyme solution for 1 hour at room temperature. After washing, slides were incubated for 10 minutes with 5 µg/ml of propidium iodide and 50 µg/ml of RNase-A in PBS at 37°C. Cells were viewed on a Zeiss Axioplan fluorescent microscope and analyzed by counting the number of normal versus apoptotic nuclei in 10 high-power fields (∼800 nuclei per condition).

Results

Effects of FTI on Anchorage-dependent Growth

Treatment with L-744,832 resulted in dose-dependent growth inhibition in all five pancreatic cancer cell lines, with considerable variation in sensitivity among the different lines (Figure 1). The Panc-1 and Capan-2 cells were most sensitive to the growth inhibitory effects of L-744,832, with IC_{50} values of 1.3 and 2.1 µM, respectively. In contrast, the IC_{50} value for Cfpac-1 cells was not reached, even at L-744,832 concentrations up to 50 µM (Table 1). L-744,832 treatment inhibited the growth of Bxpc-3 cells with moderate effectiveness, even though these cells carry only the wild-type K-Ras allele. These results are consistent with prior studies demonstrating FTI-mediated growth inhibition of tumor cell regardless of Ras mutation status [14,28].

Changes in Cell Cycle Position and Induction of Apoptosis

Flow cytometric analysis of propidium iodide-labeled cellular DNA revealed significant changes in cell cycle distribution following treatment with 10 µM L-744,832 for 72 hours (Figure 2, A and B). The most sensitive cell line, PANC-1, showed a nearly three-fold relative increase in cells with a 4N DNA population, consistent with cell cycle arrest either during G2 or during early mitosis (G2/M). In contrast, a minimal increase in G2/M fraction was observed in the resistant Cfpac-1 cell line. The other cell lines showed intermediate degrees of G2/M arrest. No evidence of FTI-induced G1 arrest was observed in any of the cell lines tested. When cell cycle distribution was analyzed as a function of L-744,832 concentration, each of the five cell lines showed a dose-dependent increase in G2/M fraction (Figure 2C). This L-744,832 dose-dependent effect was most prominent for the Panc-1 and Capan-2 cell lines and less apparent for the resistant Cfpac-1 cells, suggesting that a delay in
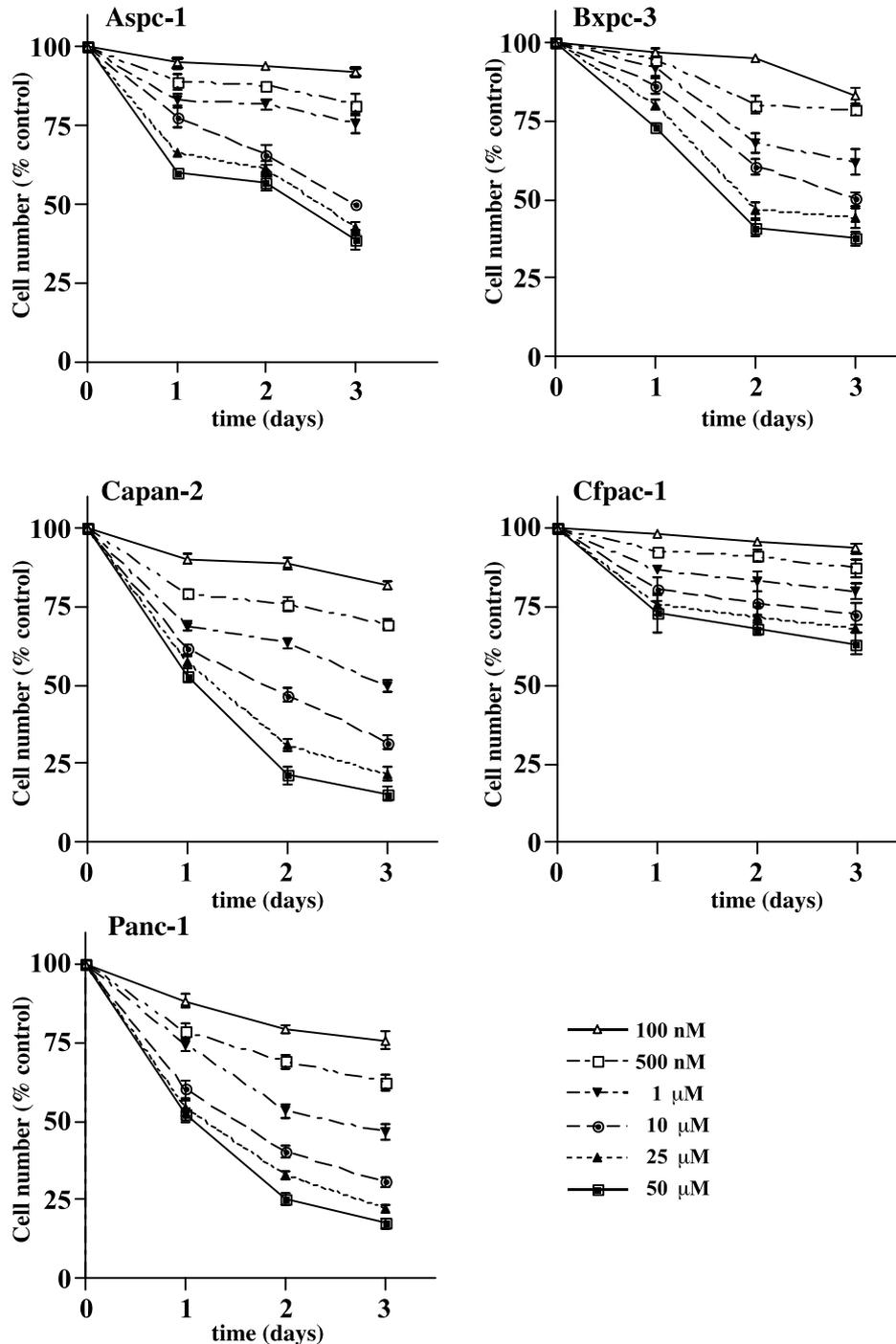
Figure 1. *Inhibition of pancreatic cancer cell growth by FTI. Five different human pancreatic cancer cell lines were treated with escalating doses of the farnesyl transferase inhibitor L - 744,832. Control cells were treated with 0.1% DMSO. Growth inhibition was determined by direct counting on days 1, 2, and 3 following initiation of treatment. The y axis indicates cell number, expressed as per cent of same day DMSO - treated control cells. The x axis indicates time in days. Values represent mean ± SEM of quadruplicate plates. Open triangles, L - 744,832 100 nM. Open squares, L - 744,832 500 nM. Closed inverted triangles, L - 744,832 1 μM. Closed circles, L - 744,832 10 μM. Closed triangles, L - 744,832 25 μM. Closed squares, L - 744,832 50 μM.*

mitotic progression might underlie the growth inhibitory effects of FTI in pancreatic cancer cells.

In addition to accumulation of a 4N DNA population, the most sensitive Panc - 1 and Capan - 2 cell lines showed an expanded subdiploid peak, suggesting increased apoptosis

(Figure 2A). Further confirmation of DNA fragmentation induced by FTI treatment was performed using morphologic evaluation of propidium iodide - labeled nuclei, as well as TdT (TUNEL) labeling (Figure 3). Cells treated with 0.1% DMSO showed normal nuclear morphology and infrequent specific

Table 1. Growth Inhibition and Induction of Apoptosis in Pancreatic Cancer Cell Lines Treated with L-744,832.

Cell Line	IC$_{50}$ L-744,832 (μM)	Apoptotic Index (%) DMSO	Apoptotic Index (%) L-744,832
Aspc-1	14.3	2.4 + 1.2	23.2 + 2.7
Bxpc-3	12.3	2.2 + 1.1	17.1 + 1.2
Capan-2	2.1	3.4 + 0.8	31.6 + 3.0
Cfpac-1	>50	3.1 + 1.3	14.5 + 1.4
Panc-1	1.3	2.7 + 1.0	50.3 + 9.5

IC$_{50}$ values indicate micromolar concentrations required to obtain 50% reduction in cell number compared to DMSO-treated control in a 72-hour anchorage-dependent growth assay. Apoptotic indices indicate fraction of TUNEL-positive cells following 72-hour treatment with 0.1% DMSO versus 10 μM L-744,832. Data indicate mean ± SEM for three independent experiments.

labeling with TdT (Table 1). Following exposure to 10 μM L-744,832 for 48 hours, all cell lines demonstrated some degree of nuclear changes indicative of apoptosis, including chromatin condensation, nuclear fragmentation, and strong TUNEL labeling. This was most apparent in the Panc-1 and Capan-2 cell lines, in which the fraction of TUNEL-positive cells following L-744,832 treatment exceeded 30% (Table 1). In contrast, the resistant Cfpac-1 cell line demonstrated a significantly lower fraction of TUNEL-positive cells following FTI treatment. These data suggest that, in addition to the observed cell cycle arrest, the growth inhibitory effects of FTI are also mediated by induction of apoptosis in pancreatic cancer cell lines. FTI-induced apoptosis appears to be a p53-independent process, occurring with high frequency in Capan-2 cells harboring a wild-type p53 as well as in Panc-1 cells lacking p53.

Effect of FTI on Cell Growth Following Ionizing Radiation

Based on previous studies suggesting a radiosensitizing effect of FTI, the effect of escalating doses of L-744,832 on Panc-1 cell growth following ionizing radiation was determined. In the absence of L-744,832 treatment, irradiated Panc-1 cells show a dose-dependent inhibition of cell growth as assessed 2 days following radiation delivery, with a radiation IC$_{50}$ dose of 4 Gy (Figure 4A). At 5 days, this radiation-induced growth inhibition was less prominent, with only those conditions involving radiation doses greater than 6 Gy showing ongoing failure to expand cell number. In contrast, cells treated with low concentrations of L-744,832 plus radiation showed additive growth inhibition, with sustained failure to expand cell number (Figure 4, A and B). For each dose of radiation studied, 0.1 μM L-744,832 was able to cause at least a 50% reduction in surviving cell number at 48 hours compared to radiation alone. These findings suggest that the combined effects of ionizing radiation and FTase inhibition result in enhanced cytotoxicity in human pancreatic cancer cells.

Effects of FTI on CyclinB1/cdc2 Kinase Activity in Irradiated and Nonirradiated Cells

To further characterize the cell cycle arrest induced by L-744,832 and evaluate possible mechanisms by which FTI

might alter cellular sensitivity to ionizing radiation, the effects of FTI on cyclinB1/cdc2 kinase activity were determined using an immunoprecipitation-based assay [26,27]. Compared to DMSO vehicle-treated control cells, all five cell lines showed enhanced cyclin B1/cdc2 kinase activity following treatment with 10 μM L-744,832 for 72 hours (Figure 5A). Paralleling observations made regarding growth inhibition and G2/M cell cycle arrest, the Panc-1 cell line demonstrated the greatest relative change, with an approximately two-fold increase in measurable cyclin B1/cdc2 kinase activity following FTI treatment for 72 hours. Enhanced kinase activity was observed in the absence of significant changes in cellular levels of cyclin B, total cdc2, or Y15-phosphorylated cdc2 as assessed by Western blot (data not shown). In spite of high levels of cyclin B1/cdc2 kinase activity, L-744,832-treated cells showed no evidence of enhanced mitotic spindle formation (see propidium iodide staining in Figure 3). These data suggest that FTI-induced G2/M cell cycle arrest occurred in early mitosis at a point downstream of cyclin B1/cdc2 kinase activation and the DNA damage-inducible G2/M cell cycle checkpoint. In addition, the results suggest that FTI may limit the ability of pancreatic cancer cells to fully initiate mitosis in response to activated cyclin B1/cdc2 kinase.

In several systems, resistance to ionizing radiation appears to correlate with downregulation of cyclin B1/cdc2 kinase activity, resulting in pre-mitotic arrest at the DNA damage-inducible G2/M cell cycle checkpoint [29,30]. To determine the effects of radiation alone compared to radiation plus FTI on cyclin B1/cdc2 kinase activity in pancreatic cancer cells, assays of kinase activity were performed following combined treatment with ionizing radiation and L-744,832. For these experiments, cells were left untreated or exposed to 8 Gy of ionizing radiation, then immediately treated with escalating doses of L-744,832 (0 to 25 μM). Fresh medium containing L-744,832 was replaced daily, and immunoprecipitatable cyclin B1/cdc2 kinase activity was measured at 8, 24, 48, and 72 hours following radiation delivery (Figure 5, B and C).

In each of the five cell lines, treatment with ionizing radiation alone induced accumulation of cells with a 4N DNA population (data not shown). This observation correlated with significant decreases in measurable cyclin B1/cdc2 kinase activity, indicating cell cycle arrest at the DNA damage-inducible G2/M cell cycle checkpoint. For Panc-1 cells, downregulation of cyclin B1/cdc2 kinase activity was most pronounced 8 hours following radiation, when cellular kinase activity was approximately 50% of nonirradiated cells (Figure 5B). This downregulation of cyclin B1/cdc2 was followed by a significant increase in activity at 24 hours (Figure 5C), possibly due to subsequent progression of a synchronized G2/M population back into the cell cycle. In the presence of low concentrations of L-744,832, radiation-induced downregulation of cyclin B1/cdc2 kinase activity was not observed. Instead, cells exposed to the combination of ionizing radiation and L-744,832 exhibited an approximate two-fold *increase* in kinase activity 8 hours following treatment, with kinase activity further increasing to levels
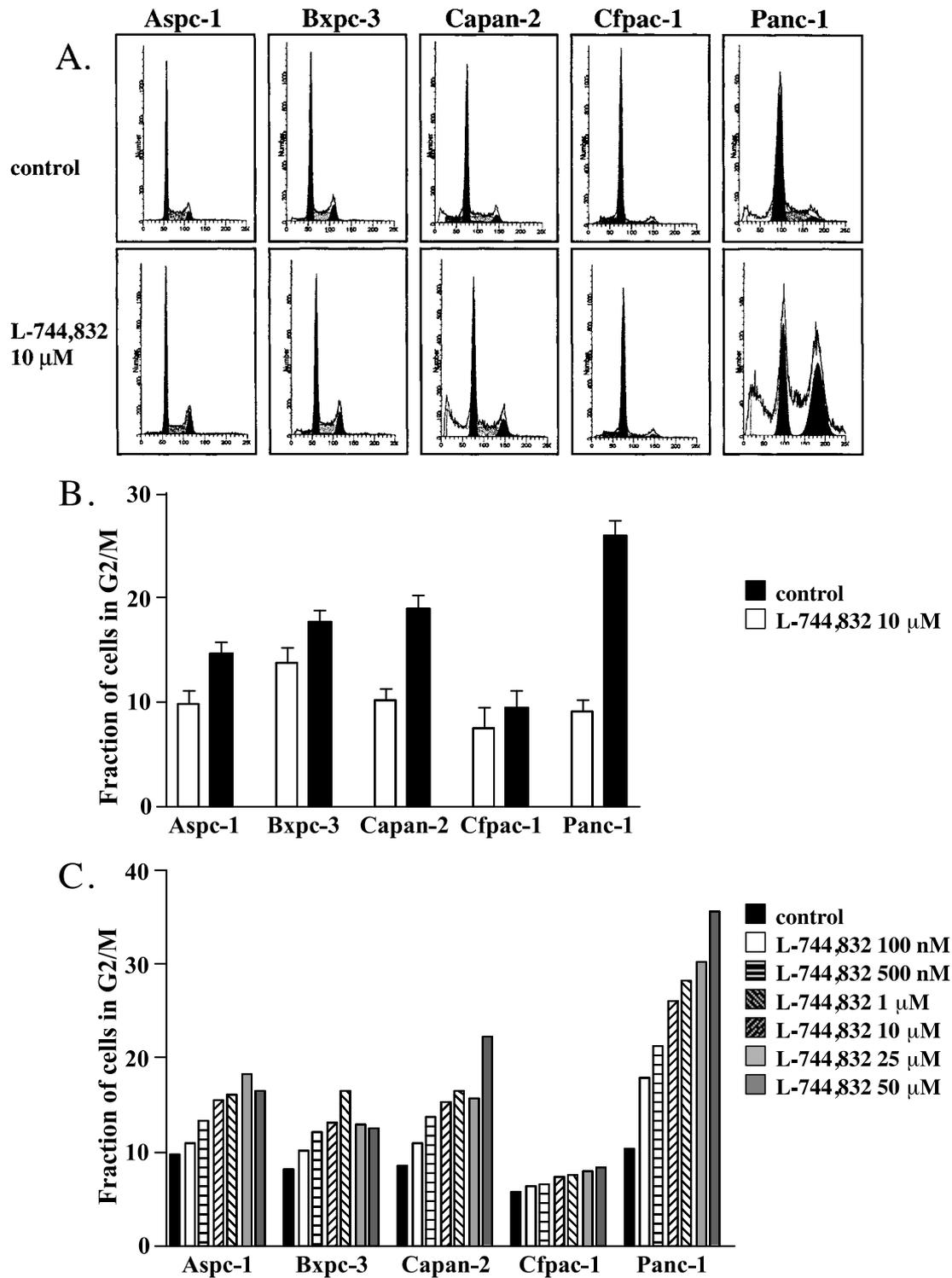
Figure 2. *Effect of FTI on cell cycle kinetics in pancreatic cancer cell lines. Five different human pancreatic cancer cell lines were treated with either L‐744,832 or 0.1% DMSO vehicle control. Cell cycle distribution was determined by propidium iodide staining and flow cytometry. (A) Cell cycle profiles of all five cell lines following treatment with 10 µM L‐744,832 for 72 hours. Upper "a" panels indicate control cells. Lower "b" panels indicate FTI‐treated cells. 1a and 1b, Aspc‐1 cells. 2a and 2b, Bxpc‐3 cells. 3a and 3b, Capan‐2 cells. 4a and 4b, Cfpac‐1 cells. 5a and 5b, Panc‐1 cells. (B) Accumulation of cells with 4N DNA population following FTI treatment. For each cell line, the fraction of cells with 4N DNA population (G2/M) was determined following treatment with 0.1% DMSO (white bars) or with 10 µM L‐744,832 (black bars) for 72 hours. Values represent mean ± SEM of three independent experiments for each condition, with each experiment involving cell cycle analysis of 10,000 cells. (C) Dose‐dependent accumulation of cells with 4N DNA population following FTI treatment. Values indicate fraction of cells with 4N DNA population (G2/M) in single representative experiment. Black bars, 0.1% DMSO. White bars, L‐744,832 100 nM. Horizontal hatched bars, L‐744,832 500 nM. Upsloping hatched bars, L‐744,832 1 µM. Downsloping hatched bars, L‐744,832 10 µM. Light grey bars, L‐744,832 25 µM. Dark grey bars, L‐744,832 50 µM.*
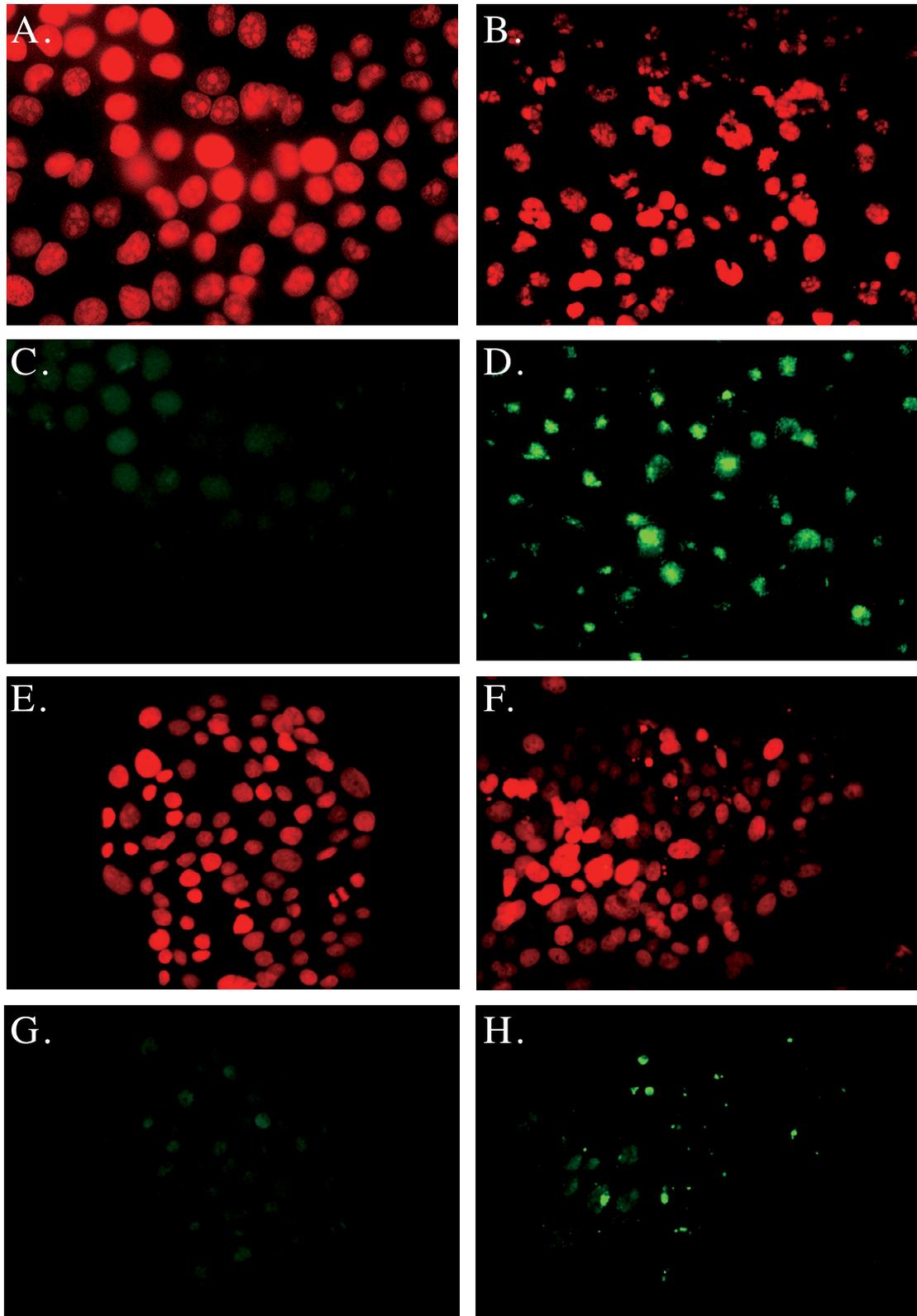
Figure 3. *Induction of apoptosis by FTI in pancreatic cancer cell lines. Cells were treated with either L - 744,832 (10 µM) or 0.1% DMSO vehicle control for 72 hours. Nuclear morphology was assessed by propidium iodide staining, and the induction of apoptosis was confirmed by TUNEL assay. (A – D) Panc - 1 cells. (E – H) Cfpac - 1 cells. (A), (B), (E), (F) Propidium iodide staining. (C), (D), (G), (H) TUNEL labeling. (A), (C), (E), (G) Cells treated with 0.1% DMSO vehicle control. (B), (D), (F), (G) Cells treated with 10 µM L - 744,832. Note nuclear fragmentation and high frequency of TUNEL positivity in FTI - treated Panc - 1 cells. Apoptotic indices from replicate experiments are provided in Table 1.*
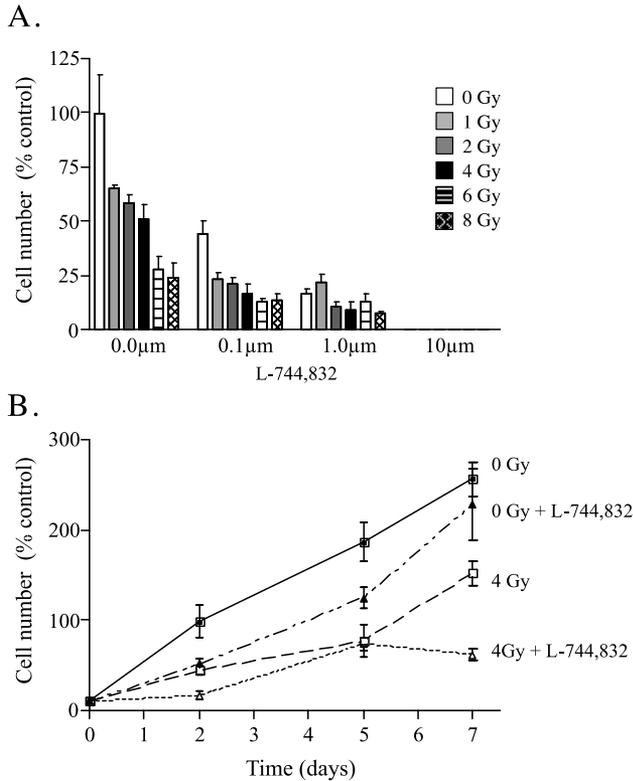
A.

B.

Figure 4. *Effect of FTI on growth inhibitory effects of ionizing radiation in Panc-1 cells. Cells were exposed to escalating doses of ionizing radiation (0 to 8 Gy) and immediately treated with 0.1% DMSO or escalating concentrations of L-744,832 (0 to 10 μM). Values indicate mean±SEM of three independent experiments. (A) Cell number on day 2 following radiation with or without simultaneous L-744,832 treatment. Y axis indicates cell number as percentage of untreated control. White bars, 0 Gy. Light grey bars, 1 Gy. Dark grey bars, 2 Gy. Black bars, 4 Gy. Horizontal hatched bars, 6 Gy. Diagonal hatched bars, 8 Gy. (B) Cell number as a function of time following radiation with or without simultaneous treatment with 1 μM L-744,832. Y axis indicates cell number as percentage of day 2 untreated control. X axis indicates time in days. Closed squares, 0 Gy + 0.1% DMSO. Closed triangles, 0 Gy + 1 μM L-744,832. Open squares, 4 Gy + 0.1% DMSO. Open triangles, 4 Gy + 1 μM L-744,832.*

five-fold over baseline at 24 and 48 hours. Concentrations of L-744,832 as low as 0.1 μM induced activation rather than downregulation of cyclin B1/cdc2 kinase activity following ionizing radiation, with no additional effect provided by higher concentrations (Figure 5C). Together, the data regarding cell cycle kinetics and mitotic kinase activation show that low-dose FTI induces cell cycle arrest at a point subsequent to the DNA damage-inducible G2/M cell cycle checkpoint before to the formation of mitotic spindles. This appears to result in a population of cells with sustained activation of cyclin B1/cdc2 kinase, even after exposure to ionizing radiation. Based on the observation that induction of apoptosis in many systems is associated with activation of cyclin B1/cdc2 kinase [26,31–34], these findings suggest that the growth inhibitory and radiation-sensitizing effects of FTI may be mediated by changes in cyclin B1/cdc2 kinase activity.

Effect of FTI on Ras Processing

To gain insight into the effects of FTI on posttranslational modification of Ras proteins, immunofluorescent staining
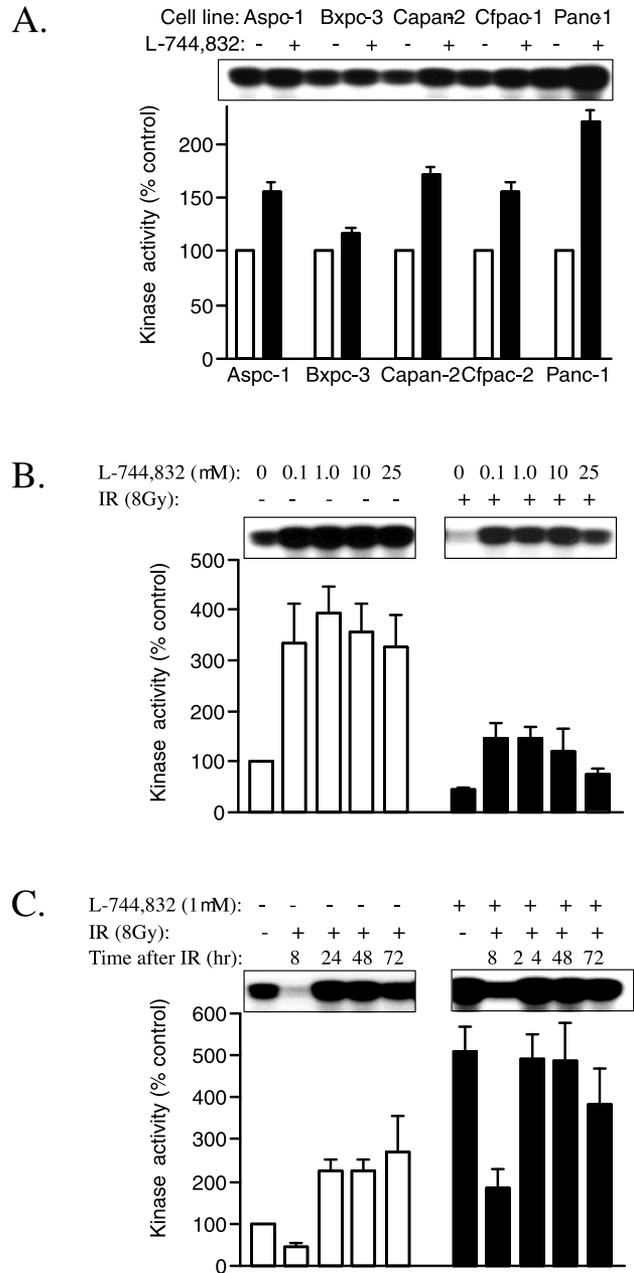
A.

B.

C.

Figure 5. *Effect of FTI on cyclin B1/cdc2 kinase activity in irradiated and nonirradiated pancreatic cancer cells. Autoradiographs depict incorporation of radioactive phosphate into histone H1 substrate. Bar graphs depict quantified kinase activity as mean±SEM of three independent experiments. (A) Effect of FTI on cyclin B1/cdc2 kinase activity in nonirradiated pancreatic cancer cell lines. Cells were treated with either L-744,832 (10 μM) or 0.1% DMSO vehicle control for 72 hours. For each cell line, data are expressed as percentage of DMSO-treated control. White bars, DMSO-treated control conditions. Black bars, L-744,832-treated cells. (B) Effect of escalating concentrations of FTI on cyclin B1/cdc2 kinase activity following ionizing radiation (IR). Panc-1 cells were exposed to 0 Gy or 8 Gy of ionizing radiation, immediately treated with 0.1% DMSO or escalating concentrations of L-744,832, and harvested 8 hours later for measurement of kinase activity. Data are expressed as percentage of nonirradiated DMSO-treated control cells. White bars, nonirradiated cells. Black bars, irradiated cells. (C) Temporal changes in cyclin B1/cdc2 kinase activity following ionizing radiation in cells treated with and without FTI. Panc-1 cells were exposed to 0 Gy versus 8 Gy of ionizing radiation, and immediately treated with 0.1% DMSO or 1 μM L-744,832. Kinase activity was determined at indicated time points. White bars, DMSO-treated cells. Black bars, L-744,832-treated cells.*

was performed using a pan-Ras primary antibody. All five cell lines were treated for 72 hours with either 10 µM L-744,832 or 0.1% DMSO. For each of the five cell lines, the pattern of pan-Ras immunofluorescence in DMSO-treated control cells was characterized by well-demarcated staining of the cytoplasmic membrane. In contrast, L-744,832-treated cells show a significant decrease in membrane staining with an increase in diffuse cytoplasmic labeling (Figure 6A). In spite of significant differences in sensitivity to the growth inhibitory effects of FTI, the degree of FTI-induced alteration in pan-Ras subcellular localization was similar in each of the five lines. These findings suggest that FTI treatment effectively prevents posttranslational processing events required for association of some or all Ras proteins with the cytoplasmic membrane, even in cell lines that are relatively resistant to the growth inhibitory effects of FTI. To further characterize the effects of FTI on processing of specific Ras-family members, immunoblot analysis was performed using H-Ras, K-Ras, and N-Ras specific antisera (Figure 6B). In each of the five cell lines examined, prenylation of H-Ras was completely inhibited in the presence of 10 µM FTI, as evidenced by shift to a more slowly migrating, unprocessed form. In contrast, no change in K-Ras processing was observed in any of the five cell lines. N-Ras processing demonstrated an intermediate effect, with the appearance of both processed and unprocessed forms induced by FTI treatment. These results are consistent with prior studies demonstrating differential sensitivity of H-Ras, K-Ras, and N-Ras to inhibition of prenylation by FTI [35,36]. In addition, the results suggest no effect on K-Ras processing by concentrations of FTI that effectively alter G2/M cell cycle regulation and induce apoptosis in sensitive cell lines.

Discussion

These findings demonstrate variable sensitivity to growth inhibition by FTI among five different human pancreatic cancer cell lines. The L-744,832 IC$_{50}$ for the various cell lines ranged from 1 to >50 µM. Sensitivity did not appear to correlate with the presence or absence of activating K-Ras mutations, as the single cell line lacking Ras mutation demonstrated intermediate sensitivity. Sensitivity did correlate with accumulation of cells exhibiting 4N DNA content and high levels of cyclin B1/cdc2 kinase activity, implying cell cycle arrest in early mitosis, downstream from the DNA damage-inducible G2/M cell cycle checkpoint. In addition, sensitivity to L-744,832 directly correlated with the induction of apoptosis, as demonstrated by the development of a subdiploid DNA population and nucleosomal DNA fragmentation. In addition to these direct effects on pancreatic cancer cell growth, low concentrations of L-744,832 additively enhanced the cytotoxic effect of ionizing radiation. The effects of L-744,832 on pancreatic cancer cell cycle regulation were associated with changes in the subcellular localization of Ras family members and inhibition of H-Ras and N-Ras processing; however, an effect on the post-translational processing of K-Ras was not observed.

Together, these findings suggest that FTase inhibition directly influences pancreatic cancer cell growth and survival, and that these effects may be mediated by significant changes in G2/M cell cycle progression. The relevant prenylated protein targets responsible for these effects remain to be identified.

The current results are consistent with previous studies demonstrating effective growth inhibition of a wide variety of human tumor cell lines by L-744,832 and other FTase inhibitors [14,28,37]. Several studies have previously suggested an effect of FTIs on pancreatic cancer cell growth [14,37,38]. Using assays of anchorage-independent growth in soft agar, Sepp-Lorenzino and colleagues previously reported L-744,832 IC$_{50}$ values of less than 20 µM for Capan-2 cells, but greater than 20 µM for the Panc-1 and Aspc-1 cell lines [14]. Similar to our findings, other investigators using different inhibitors of posttranslational prenylation have demonstrated effective growth inhibition in pancreatic cancer cell lines regardless of K-Ras mutation status [38,39].

Both in pancreatic cancer cell lines [38], as well as in other systems [37,40–42], the growth inhibitory effects of FTase inhibition have previously been associated with the induction of apoptosis. In the current study, FTI-induced apoptosis appeared to represent a p53-independent event, with all cell lines except Capan-2 lacking a functional p53 allele. Similarly, Lebowitz and coworkers [40] demonstrated that the ability of FTI to induce apoptosis as opposed to simple morphologic reversion was dependent on substratum adherence, and was unaffected by the presence or absence of p53 mutation. These findings are consistent with those of Barrington et al., who noted that L-744,832 retained its ability to induce tumor cell apoptosis in MMTV-v-Ha-Ras/p53−/− mice, albeit with somewhat lower efficacy compared to a MMTV-v-Ha-Ras/p53+/+ background [41]. In contrast, the ability of L-744,832 to inhibit in vivo tumor growth in MMTV-v-Ha-Ras/MMTV-c-myc mice was not associated with a statistically significant increase in tumor cell apoptotic index, suggesting that the effects of FTI on in vivo tumor cell growth may be mediated by both apoptotic and non-apoptotic mecha-nisms [41].

Previous investigations have not addressed the effects of FTase inhibition on cell cycle regulation in pancreatic cancer cells. In other cell systems, inhibition of G1-S transit appears to be the predominant cell cycle effect induced by FTI [28,37,41]. Whereas FTI induces apoptosis in a p53-independent manner, FTI-induced G1 cell cycle arrest appears to be dependent on both p53 and p21$^{WAF1/CIP1}$ [28]. When either p53 or p21$^{WAF1/CIP1}$ are absent, the antiproliferative effects of FTI are instead mediated by the development of polyploidy (endoreduplication) and the induction of apoptosis [28]. These results using genetically targeted cell systems are consistent with the present results, in which no evidence of FTI-mediated G1 arrest was noted in any of the five pancreatic cancer cell lines studied. Four of these lines have been documented to have homozygous inactivating mutations in p53, whereas wild-type p53 sequence has previously been reported in Capan-2 cells
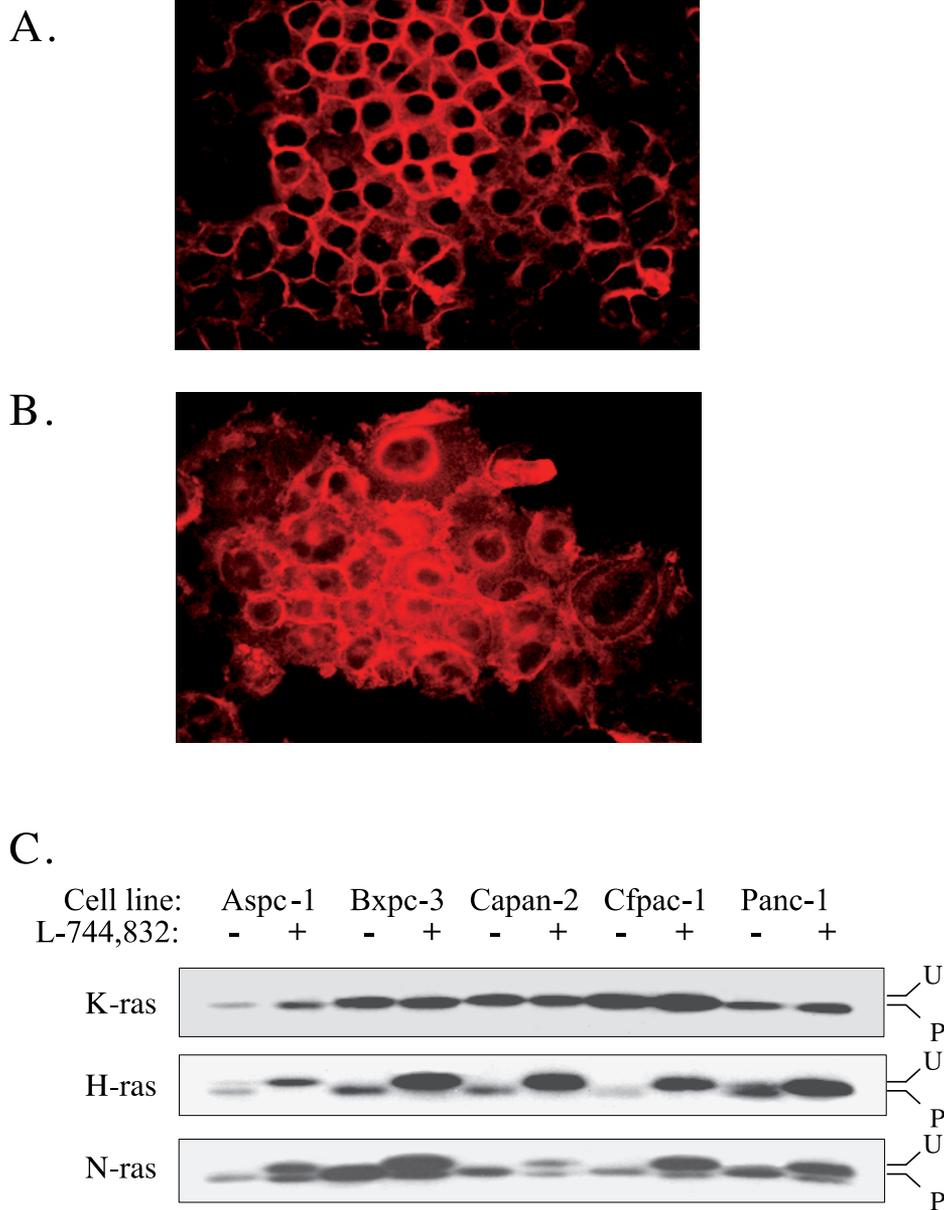
A.

B.

C.

Figure 6. *Effect of FTI on subcellular localization and posttranslational processing of ras proteins. (A) Pan-ras immunoreactivity in Panc-1 cells treated with 0.1% DMSO for 72 hours. Note predominant staining of cytoplasmic membrane. (B) Pan-ras immunoreactivity in Panc-1 cells treated with 10 µM L-744,832 for 72 hours. Increased cytoplasmic staining is noted. (C) Immunoblot analysis of FTI-induced changes in posttranslational processing of Ras proteins. Cells were treated with 0.1% DMSO versus 10 µM L-744,832 for 72 hours. "U" indicates unprocessed upper band. "P" indicates processed lower band. Results are representative of two independent experiments.*

[24,25]. However, we did not observe p21$^{WAF1/CIP1}$ induction or G1 checkpoint arrest following DNA damage in this line, suggesting functional disruption of the p53 pathway in these cells (data not shown). Although our gated flow cytometric analysis did not detect obvious endoreduplication in pancreatic cancer cells following FTI treatment, the accumulation of cells with a 4N DNA population in conjunction with high levels of cyclin B1/cdc2 kinase is consistent with this interpretation [27]. A previous report demonstrating FTI-induced accumulation of a 4N DNA population in the A549 human lung cancer cell line [43] suggests that this may represent a common response in tumor cells with disrupted G1 checkpoint regulation.

The current study also uniquely correlates sensitivity to FTI with accumulation of activated cyclin B1/cdc2 kinase in both irradiated and nonirradiated cells. In eukaryotic cells, regulation of cyclin B1/cdc2 kinase activity plays a critical role in regulating normal mitotic entry as well as the DNA damage-inducible G2/M cell cycle checkpoint. In addition, activation of cyclin B1/cdc2 kinase has also been associated with induction of apoptosis [26,31–34,44]. In the current study, the ability of FTI to induce early mitotic arrest,

activation of cyclin B1/cdc2 and induction of apoptosis resembles the effect of taxol and other microtubule inhibitors [27,44]. As in the case of FTI treatment, cell fate following treatment with microtubule inhibitors appears to depend on the presence or absence of intact G1/S checkpoint mechanisms. Stewart and colleagues [27] have demonstrated prolonged cyclin B1/cdc2 kinase activation and enhanced apoptosis following taxol treatment in HCT116 $p21-/-$ cells compared to a HCT116 $p21+/+$ parental strain. The introduction of ectopic p21$^{WAF1/CIP1}$ has also been shown to limit cyclin B1/cdc2 kinase activity and decrease the sensitivity of p53-deficient tumor cells to induction of apoptosis in response to microtubule inhibitors [27,44].

A common mechanism ultimately involving activation of cyclin B1/cdc2 may therefore be responsible for p53-independent induction of apoptosis by either FTI or microtubule inhibitors. Additional evidence suggests that combined treatment with FTI and a microtubule inhibitor may generate synergistic effects with respect to accumulation of a 4N DNA population [45,46] and initiation of apoptosis [46,47]. The results of the current study suggest that this effect may be mediated by enhanced cyclin B1/cdc2 kinase activity. This mechanism may also underlie the additive increase in cytotoxicity associated with combined radiation plus FTI compared to radiation alone. In this regard, G2/M has previously been characterized as the most sensitive phase of the cell cycle with respect to the cytotoxic effects of ionizing radiation [48,49]. Taxol-induced G2/M arrest also increases cellular sensitivity to ionizing radiation, apparently related to changes in cyclin B1/cdc2 kinase activity [50,51]. In the current study, simultaneous treatment with ionizing radiation and 1 µM L-744,832 resulted in a rapid increase in cyclin B1/cdc2 activity compared to untreated control cells, as opposed to the downregulation of kinase activity observed following radiation alone. In this regard, both FTI and microtubule inhibitors appear to override the cytoprotective DNA damage-inducible G2/M cell cycle checkpoint, resulting in enhanced cytotoxicity.

Together, these results suggest that farnesylated proteins may be involved in regulation of mitotic entry and progression. However, the identity of the farnesylated proteins responsible for the effects of FTI in pancreatic cancer cells remain unknown. In the current study, biochemical analysis failed to demonstrate any apparent effect on the posttranslational processing of K-Ras, even while H-Ras and N-Ras showed evidence of impaired posttranslational prenylation. Similar results have been observed in other systems, in which K-Ras appears to be relatively resistant to the effects of FTI, apparently due to a high affinity for FTase as well as alternative prenylation by GGTase-I [35,36,52]. FTI treatment has also been shown to alter farnesylation of nuclear lamins [14,53], although the impact of this effect on cell cycle regulation remains unknown.

In contrast, an expanding body of evidence suggests that the growth inhibitory properties of FTI are mediated by effects on the RhoB small GTPase protein [40,54–58]. Using myristylated forms of H-Ras and RhoB that are resistant to the effects of FTI, Lebowitz and colleagues demonstrated that myristylated RhoB, but not myristylated H-Ras, rendered Ras-transformed cells resistant to the growth inhibitory effects of FTI [40,56]. Additional studies have suggested that the effects of FTI on RhoB involve loss of farnesylated RhoB and a gain of alternatively geranylgeranylated RhoB [57,58]. Similar to the effects of FTI, geranylgeranylated RhoB is capable of activating p21$^{WAF1/CIP1}$ in Ras-transformed cells with wild-type p53 [57], and also capable of causing accumulation of cells with a 4N DNA content in certain tumor lines with mutant p53 [58]. Based on the results of the current study, it might be predicted that, in the absence of wild-type 53, cells with predominantly geranylgeranylated RhoB would also demonstrate high levels of cyclin B1/cdc2 kinase activity.

References
[1] Zhang FL, and Casey PJ (1996). Protein prenylation: molecular mechanisms and functional consequences. *Annu Rev Biochem* **65**, 241–269.
[2] Gibbs JB, and Oliff A (1997). The potential of farnesyltransferase inhibitors as cancer chemotherapeutics. *Annu Rev Pharmacol Toxicol* **37**, 143–166.
[3] Armstrong SA, Hannah VC, Goldstein JL, and Brown MS (1995). CAAX geranylgeranyl transferase transfers farnesyl as effeciently as geranylgeranyl to RhoB. *J Biol Chem* **270**, 7864–7868.
[4] James GL, Goldstein JL, and Brown MS (1995). Polylysine and CVIM sequences of K-RasB dictate specificity of prenylation and confer resistance to benzodiazepine peptidomimetic *in vitro*. *J Biol Chem* **270**, 6221–6226.
[5] Andres AD, Seabra MC, Brown MS, Armstrong SA, Smeland TE, Cremers FPM, and Goldstein JL (1993). cDNA cloning of component A of Rab geranylgeranyltransferase and demonstration of its role as a Rab escort protein. *Cell* **73**, 1091–1099.
[6] Barbacid M (1987). Ras genes. *Annu Rev Biochem* **56**, 779–827.
[7] Boguski MS, and McCormick F (1993). Proteins regulating ras and its relatives. *Nature* **366**, 643–654.
[8] Hruban RH, Van Mansfeld ADM, Offerhaus GJ, *et al.* (1993). K-ras oncogene activation in adenocarcinoma of the human pancreas. *Am J Pathol* **143**, 545–554.
[9] Almoguera C, Shibata D, Forrester K, *et al.* (1988). Most human carcinomas of the exocrine pancreas contain mutant c-K-ras genes. *Cell* **53**, 549–554.
[10] Schafer WR, Kim R, Sterne R, Thorner J, Kim S-H, *et al.* (1989). Genetic and pharmacologic suppression of oncogenic mutations in RAS genes of yeast and humans. *Science* **245**, 379–385.
[11] Stokoe D, Macdonald SG, Cadwallader K, Symons M, and Hancock JF (1994). Activation of Raf as a result of recruitment to the plasma membrane. *Science* **264**, 1463–1467.
[12] Gibbs JB, Oliff A, and Kohl NE (1994). Farnesyltransferase inhibitors: Ras research yields potential cancer therapeutic. *Cell* **77**, 175–178.
[13] Lobell RB, and Kohl NE (1998). Pre-clinical development of farnesyltransferase inhibitors. *Cancer Metastasis Rev* **17**, 203–210.
[14] Sepp-Lorenzino L, Ma Z, Rands E, Kohl NE, Gibbs JB, Oliff A, and Rosen N (1995). A peptidomimetic inhibitor of farnesyl:protein transferase blocks the anchorage-dependent and -independent growth of human tumor cell lines. *Cancer Res* **55**, 5302–5309.
[15] Kohl NE, Mosser SD, deSolms SJ, Giuliani EA, Pompliano DL, Graham SL, Smith RL, Scolnick EM, Oliff A, and Gibbs JB (1993). Selective inhibition of ras-dependent transformation by a farnesyltransferase inhibitor. *Science* **260**, 1934–1937.
[16] James GL, Goldstein JL, Brown MS, Rawson TE, Somers TC, McDowell RS, Crowley CW, Lucas BK, Levinson AD, and Marsters

JC Jr (1993). Benzodiazepine peptidomimetics: potent inhibitors of Ras farnesylation in animal cells. *Science* **260**, 1937–1942.

[17] Kohl NE, Wilson FR, Mosser SD, Giuliani E, DeSolms SJ, Conner MW, Anthony NJ, Holtz WJ, Gomez RP, Lee TJ, Smith RL, Grahm SL, Hartman GD, Gibbs JB, and Oliff A (1994). Protein farnesyltransferase inhibitors block the growth of ras-dependent tumors in nude mice. *Proc Natl Acad Sci USA* **91**, 9141–9145.

[18] Kohl NE, Omer CA, Conner MW, Davide JP, Anthony NJ, deSolms SJ, Guiliani EA, Gomez RP, Graham SL, Hamilton K, Handt LK, Hartman GD, Koblan KS, Kral AM, Miller PJ, Mosser SM, O'Neill TJ, Rands E, Schaber ME, Gibbs JB, and Oliff A (1995). Inhibition of farnesyl-transferase induces regression of mammary and salivary carcinomas in ras transgenic mice. *Nat Med* **1**, 792–797.

[19] Landis SH, Murray T, Bolden S, and Wingo PA (1998). Cancer statistics, 1998. *CA-Cancer J Clin* **48**, 6–29.

[20] Leach SD (1998). Resectable pancreatic adenocarcinoma: strategies to improve local tumor control. In *Pancreatic Cancer: Molecular and Clinical Management Prospects*, F Sarkar and M Dugan (Eds). Eaton Publishing, Natick, MA, pp. 145–156.

[21] Carter G, Gilbert C, and Lemoine NR (1995). Effects of antisense oligonucleotides targeting K-ras expression in pancreatic cancer cell lines. *Int J Oncol* **6**, 1105–1112.

[22] Shichinohe T, Senmaru N, Furuuchi K, *et al.* (1996). Suppression of pancreatic cancer by the dominant negative ras mutant, N116Y. *J Surg Res* **66**, 125–130.

[23] Leach SD, Berger DH, Davidson BS, *et al.* (1998). Enhanced Krev-1 expression inhibits the growth of pancreatic adenocarcinoma cells. *Pancreas* **16**, 491–498.

[24] Redston MS, Caldas C, Seymour AB, Hruban RH, da Costa L, Yeo CJ, and Kern SE (1994). p53 mutations in pancreatic carcinoma and evidence of common involvement of homocopolymer tracts in DNA microdeletions. *Cancer Res* **54**, 3025–3033.

[25] Caldas C, Hahn SA, da Costa LT, *et al.* (1994). Frequent somatic mutations and homozygous deletions of the p16 (MTS1) gene in pancreatic adenocarcinoma. *Nat Genet* **8**, 27–32.

[26] Leach SD, Scatena CD, Keefer CJ, Goodman HA, Song SY, Yang L, and Pietenpol JA (1998). Negative regulation of Wee1 expression and Cdc2 phosphorylation during p53-mediated growth arrest and apoptosis. *Cancer Res* **58**, 3231–3236.

[27] Stewart ZA, Leach SD, and Pietenpol JA (1999). p21$^{Waf1/Cip1}$ inhibition of cyclin E/Cdk2 activity prevents endoreduplication after miotic spindle disruption. *Mol Cell Biol* **19**, 205–215.

[28] Sepp-Lorenzino L, and Rosen N (1998). A farnesyl-protein transferase inhibitor induces p21 expression and G1 block in p53 wild type tumor cells. *J Biol Chem* **273**, 20243–20251.

[29] Rhind N, Furnari B, and Russell P (1997). Cdc2 tyrosine phosphorylation is required for the DNA damage checkpoint in fission yeast. *Genes Dev* **11**, 504–511.

[30] O'Connell MJ, Raleigh JM, Verkade HM, and Nurse P (1997). Chk1 is a Wee1 kinase in the G2 DNA damage checkpoint inhibiting Cdc2 by Y15 phosphorylation. *EMBO J* **16**, 545–554.

[31] Shi L, Nishioka WK, Th'ng J, Bradbury EM, Litchfield DW, and Greenberg AH (1994). Premature p34^{Cdc2} activation required for apoptosis. *Science* **263**, 1143–1145.

[32] Shimizu T, O'Connor PM, Kohn KW, and Pommier Y (1995). Unscheduled activation of cyclin B1/Cdc2 kinase in human promyelocytic leukemia cell line HL60 cells undergoing apoptosis induced by DNA damage. *Cancer Res* **55**, 228–231.

[33] Fotedar R, Flatt J, Gupta S, Margolis RL, Fitzgerald P, Messier H, and Fotedar A (1995). Activation-induced T-cell death is cell cycle dependent and regulated by cyclin B. *Mol Cell Biol* **15**, 932–942.

[34] Yao S, McKenna KA, Sharkis SJ, and Bedi A (1996). Requirement of p34^{Cdc2} kinase for apoptosis mediated by the Fas/APO-1 receptor and interleukin 1β-converting enzyme-related proteases. *Cancer Res* **56**, 4551–4555.

[35] James G, Goldstein JL, and Brown MS (1996). Resistance of K-rasB^{V12} proteins to farnesyltransferase inhibitors in rat1 cells. *Proc Natl Acad Sci USA* **93**, 4454–4458.

[36] Fiordalisi JJ, Rushton BC, Toussaint LG, Johnson RL, and Cox AD (1999). High affinity for Ftase and alternative prenylation contribute individually to K-ras resistance to FTIs. *Proc Am Assoc Cancer Res* **40**, 521.

[37] Liu M, Bryant MS, Chen J, Lee S, Yaremko B, Lipari P, Malkowski M, Ferrari E, Nielsen L, Prioli N, Dell J, Sinha D, Syed J, Korfmacher WA, Nomeir AA, Lin CC, Wang L, Taveras AG, Doll RJ, Njoroge FG, Mallams AK, Remiszewski S, Catino JJ, Girijavallabhan VM, and Bishop WR (1998). Antitumor activity of SCH 66336, an orally bioavailable tricyclic inhibitor of farnesyl protein transferase, in human tumor xenograft models and wap-ras transgenic mice. *Cancer Res* **58**, 4947–4956.

[38] Ura H, Obara T, Shudo R, Itoh A, Tanno S, Fujii T, Nishino N, and

[39] Kohgo Y (1998). Selective cytotoxicity of farnesylamine to pancreatic carcinoma cells and Ki-ras-transformed fibroblasts. *Mol Carcinog* **21**, 93–99.

[39] Sumi S, Beauchamp RD, Townsend CM Jr, Pour PM, Ishizuka J, and Thompson JC (1994). Lovastatin inhibits pancreatic cancer growth regardless of RAS mutation. *Pancreas* **9**, 657–661.

[40] Lebowitz PF, Sakamuro D, and Prendergast GC (1997). Farnesyl transferase inhibitors induce apoptosis of ras-transformed cells denied substratum attachment. *Cancer Res* **57**, 708–713.

[41] Barrington RE, Subler MA, Rands E, Omer CA, Miller PJ, Hundley JE, Koester SK, Troyer DA, Bearss DJ, Conner MW, Gibbs JB, Hamilton K, Koblan KS, Mosser SD, O'Neill TJ, Schaber MD, Senderak ET, Windle JJ, Oliff A, and Kohl NE (1998). A farnesyltransferase inhibitor induces tumor regression in transgenic mice harboring multiple oncogenic mutations by mediating alterations in both cell cycle control and apoptosis. *Mol Cell Biol* **18**, 85–92.

[42] Norgaard P, Law B, Joseph H, Page DL, Shyr Y, Mays D, Pietenpol JA, Kohl NE, Oliff A, Coffey RJ Jr, Poulsen HS, and Moses HL (1999). Treatment with farnesyl-protein transferase inhibitor induces regression of mammary tumors in transforming growth factor (TGF) alpha and TGF alpha/neu transgenic mice by inhibition of mitogenic activity and induction of apoptosis. *Clin Cancer Res* **5**, 35–42.

[43] Miquel K, Pradines A, Sun J, Qian Y, Hamilton AD, Sebti SM, and Favre G (1997). GGTI-298 induces G0–G1 block and apoptosis whereas FTI-277 causes G2-M enrichment in A549 cells. *Cancer Res* **57**, 1846–1850.

[44] Stewart ZA, Mays D, and Pietenpol JA (1999). Defective G1-S cell cycle checkpoint function sensitizes cells to microtubule inhibitor-induced apoptosis. *Cancer Res* **59**, 3831–3837.

[45] Suzuki N, Del Villar K, and Tamanoi F (1998). Farnesyltransferase inhibitors induce dramatic morphological changes of KNRK cells that are blocked by microtubule interfering agents. *Proc Natl Acad Sci USA* **95**, 10499–10504.

[46] Ranganathan S, McCauley RA, and Hudes GR (1999). Combined cell cycle and cytotoxic effects of paclitaxel and R115777, a specific inhibitor of p21 ras function and protein farnesylation in human prostate and breast carcinoma cell lines. *Proc Am Assoc Cancer Res* **40**, 523.

[47] Moasser MM, Sep-Lorenzino L, Kohl NE, Oliff A, Balog A, Su DS, Danishefsky SJ, and Rosen N (1998). Farnesyl transferase inhibitors cause enhanced mitotic sensitivity to taxol and epothilones. *Proc Natl Acad Sci USA* **95**, 1369–1374.

[48] Terasima R, and Tolmach LJ (1963). X-ray sensitivity and DNA synthesis in synchronous populations of HeLa cells. *Science* **140**, 490–492.

[49] Sinclair WK, and Morton RA (1966). X-ray sensitivity during the cell generation cycle of cultured Chinese hamster cells. *Radiat Res* **29**, 450–457.

[50] Gorodetsky R, Levdansky L, Ringel I, and Vexler A (1998). Paclitaxel-induced modification of the effects of radiation and alterations in the cell cycle in normal and tumor mammalian cells. *Radiat Res* **150**, 283–291.

[51] Tishler RB, Geard CR, Hall EJ, and Schiff PB (1992). Taxol sensitizes human astrocytoma cells to radiation. *Cancer Res* **52**, 3495–3497.

[52] Whyte DB, Kirschmeier P, Hockenberry TN, Nunez-Oliva I, James L, Catino JJ, Bishop WR, and Pai JK (1997). K- and N-Ras are geranylgeranylated in cells treated with farnesyl protein transferase inhibitors. *J Biol Chem* **272**, 14459–14564.

[53] Dalton MB, Fantle KS, Bechtold HA, DeMaio L, Evans RM, Krystosek A, and Sinensky M (1995). The farnesyl protein transferase inhibitor BZA-5B blocks farnesylation of nuclear lamins and p21ras but does not affect their function or localization. *Cancer Res* **55**, 3295–3304.

[54] Lebowitz PF, and Prendergast GC (1998). Non-ras targets of farnesyltransferase inhibitors: focus on Rho. *Oncogene* **17**, 1439–1445 (11 reviews).

[55] Prendergast GC, Davide JP, DeSolms SJ, Giuliani EA, Graham SL, Gibbs JB, Oliff A, and Kohl NE (1994). Farnesyltransferase inhibition causes morphological reversion of ras-transformed cells by a complex mechanism that involves regulation of the actin cytoskeleton. *Mol Cell Biol* **14**, 4193–4202.

[56] Lebowitz PF, Davide JP, and Prendergast GC (1995). Evidence that farnesyltransferase inhibitors suppress ras transformation by interfering with Rho activity. *Mol Cell Biol* **15**, 6613–6622.

[57] Du W, Lebowitz PF, and Prendergast GC (1999). Cell growth inhibition by farnesyltransferase inhibitors is mediated by gain of geranylgeranylated RhoB. *Mol Cell Biol* **19**, 1831–1840.

[58] Du W, and Predergast GC (1999). Geranylgeranylated RhoB mediates suppression of human tumor cell growth by farnesylated inhibitors. *Cancer Res* **59**, 5492–5496.